

Gamma Ray Emission From A Baryonic Dark Halo ‡

F De Paolis†, G Ingrassio†, Ph Jetzer‡ § and M Roncadelli¶

† Dipartimento di Fisica, Università di Lecce and INFN, Sezione di Lecce, CP 193, I-73100 Lecce, Italy

‡ Paul Scherrer Institute, Laboratory for Astrophysics, CH-5232 Villigen PSI, and Institute of Theoretical Physics, University of Zurich, Winterthurerstrasse 190, CH-8057 Zurich, Switzerland

¶ INFN, Sezione di Pavia, Via Bassi 6, I-27100, Pavia, Italy

Abstract. A re-analysis of EGRET data by Dixon et al. [1] has led to the discovery of a statistically significant diffuse γ -ray emission from the galactic halo. We show that this emission can naturally be accounted for within a previously-proposed model for baryonic dark matter, according to which dark clusters of brown dwarfs and cold self-gravitating H_2 clouds populate the outer galactic halo and can show up in microlensing observations. Basically, cosmic-ray protons in the galactic halo scatter on the clouds clumped into dark clusters, giving rise to the observed γ -ray flux. We derive maps for the corresponding intensity distribution, which turn out to be in remarkably good agreement with those obtained by Dixon et al. [1]. We also address future prospects to test our predictions.

1. Introduction

Observations of the diffuse γ -ray emission during the last twenty years || have been successfully interpreted in terms of a two-folded structure

- ★ a highly anisotropic component strongly concentrated along the galactic disk,
- ★ an apparently isotropic component.

While the former is evidently galactic in nature - being actually accounted for by cosmic ray (CR) interactions in the interstellar medium (ISM) [3] - the origin of the latter still remains an open problem in high-energy astrophysics (see e.g. [1, 4, 5]). We will restrict our attention to the latter component throughout the present paper.

‡ We would like to dedicate this work to the memory of Dennis W. Sciama

§ To whom correspondence should be addressed.

|| A comprehensive account of these matters as well as of their theoretical explanations can be found in [2].

We begin by recalling that EGRET observations have detected a diffuse γ -ray flux [6]

$$\Phi_\gamma(E_\gamma > 0.1\text{GeV}) = (1.45 \pm 0.05) \times 10^{-5} \text{ } \gamma \text{ cm}^{-2} \text{ s}^{-1} \text{ sr}^{-1} , \quad (1)$$

with a spectral slope of -2.10 ± 0.03 , which - for $E_\gamma > 1 \text{ GeV}$ - gives

$$\Phi_\gamma(E_\gamma > 1\text{GeV}) = (1.14 \pm 0.04) \times 10^{-6} \text{ } \gamma \text{ cm}^{-2} \text{ s}^{-1} \text{ sr}^{-1} . \quad (2)$$

A question naturally arises. Where does the γ -ray emission in question come from? No doubt, its characteristic isotropy calls for an extragalactic origin - an option which is further supported by the fact that it fits remarkably well with the extragalactic hard X-ray background [7].

The next question to address is whether the considered γ -ray background arises from a truly diffuse process or rather from the contribution of very many unresolved point sources. Either option has received considerable attention. Among the theories of diffuse origin are a baryon-symmetric Universe [8], primordial black hole evaporation [9, 10], early collapse of supermassive black holes [11], a new population of Geminga-like pulsars [12] and WIMP (Weakly Interacting Massive Particle) annihilation (see e.g. [13]). Models based on discrete source contribution include a variety of possibilities. What is clear since a long time is that normal galaxies fail to account for the observed isotropic background - at least as long as their disk emission is considered [14]-[17] - since the corresponding intensity falls shorter by a factor ~ 10 with respect to the detected flux. A more realistic option is provided by active galaxies [18, 19]. Indeed, blazars seem to yield a successful explanation of the isotropic γ -ray emission [20]-[24]. Finally, a somewhat hybrid model has recently been proposed, in which the isotropic γ -ray background is produced in clusters of galaxies through the interaction of CRs with the hot intracluster gas [25]. However, this model has been severely criticized [26, 27]. In fact, it gives rise to a γ -ray spectral index in disagreement with the observed one and relies upon a value for the CR density in the intracluster space which is too high to be plausible. More generally, it has been shown that the contribution to the isotropic γ -ray emission from clusters of galaxies is negligible [27].

Recently, Dixon et al. [1] have re-analyzed the EGRET data concerning the diffuse γ -ray flux with a wavelet-based technique, using the expected (galactic plus isotropic) emission as a null hypothesis. Although the wavelet approach does not allow for a good estimate of the errors, they find a statistically significant diffuse emission from an extended halo surrounding the Milky Way. This emission traces a somewhat flattened halo and its intensity at high-galactic latitude is [1]

$$\Phi_\gamma(E_\gamma > 1\text{GeV}) \simeq 10^{-7} - 10^{-6} \text{ } \gamma \text{ cm}^{-2} \text{ s}^{-1} \text{ sr}^{-1} . \quad (3)$$

Clearly, the comparison of eqs. (2) and (3) entails that the newly discovered halo γ -ray flux is a relevant fraction of the standard isotropic diffuse emission (at least for $E_\gamma > 1$

GeV).

Our aim is to show that the observed halo γ -ray emission naturally arises within a previously-proposed model for baryonic dark matter, according to which dark clusters of brown dwarfs and cold self-gravitating H_2 clouds populate the outer galactic halo and can show up in microlensing observations [28]-[32]. Basically, CR protons in the galactic halo scatter on the clouds clumped into dark clusters, giving rise to the newly discovered γ -ray flux.

Although we already pointed out that a signature of the model is a diffuse γ -ray emission from the galactic halo [28, 29], a more thorough study is required to compare the predicted intensity distribution with the observed one. A short account of these results has been presented elsewhere [33]. In the present paper, we provide a more exhaustive analysis. In addition, we estimate the γ -ray emission from the nearby M31 galaxy.

The paper is organized as follows. In Section 2 we recall the main features of our model for baryonic dark matter in the galactic halo. In Section 3 we address the CR confinement in the galactic halo and we estimate the CR energy density. In Section 4 we compute the halo γ -ray flux - produced by the clouds clumped into dark clusters through proton-proton scattering - as detected on Earth. Section 5 is devoted to the study of the γ -ray flux due to Inverse Compton (IC) scattering of electrons off background photons. In Section 6 we present γ -ray intensity maps, pertaining to both proton-proton scattering and IC scattering, and discuss their interplay. Finally, in Section 7 we address future prospects to test our predictions.

2. Dark clusters in the galactic halo

Ever since the discovery that standard big-bang nucleosynthesis correctly accounts for the light element abundances, a lesson has become clear: most of the baryons in the Universe happen to be in nonluminous form, thereby making a strong case for baryonic dark matter.

In order to see how this comes about, we recall that the fraction of critical density contributed by luminous matter is estimated to be $\Omega_L \sim 0.005$ [34] †. Yet, agreement between the predicted and observed abundances of nucleosynthetic yields is achieved only provided the similar contribution from baryons - in whatever form - lies in the range $0.01 \lesssim \Omega_B \lesssim 0.05$ [35]. Actually, this conclusion has recently been sharpened by deuterium measurements in Quasi Stellar Object (QSO) absorption spectra, which probe regions of space much farther away than previously explored and give $\Omega_B \simeq 0.05$ [36]. So, about 90% of the baryonic matter in the Universe is expected to be dark.

† We are using throughout the presently favoured value of the Hubble constant $H_0 \simeq 70 \text{ km s}^{-1} \text{ Mpc}^{-1}$.

Needless to say, one is naturally led to wonder about the distribution and form of baryonic dark matter.

Several possibilities have been contemplated over the last few years. Although no logically compelling reason in favour of any particular option has emerged so far, it looks intriguing that a naturalness argument strongly suggests that the galactic dark halos should be predominantly baryonic.

Basically, the idea is as follows. As is well known, both optical and HI observations have shown that all galactic rotation curves exhibit a universal qualitative behaviour: after a steep rise corresponding to the bulge, they stay approximately constant out to the last measured point. This feature – namely the lack of a keplerian fall-off – provides a stark evidence in favour of a spheroidal dark halo surrounding the luminous part of any galaxy. This is however not the end of the story. For, rotation curves trace the luminous – hence baryonic – matter within the optical disk, but are dominated by the halo dark matter at larger galactocentric distances. Yet, both contributions invariably turn out to match smoothly and exactly, thereby signalling a striking visible-invisible conspiracy (also called disk-halo conspiracy). Before proceeding further, a point should be stressed. With only a rather limited sample of available rotation curves, that conspiracy was initially understood as a fine-tuning whereby the disk and the halo of spiral galaxies manage to produce a flat rotation curve [37]. Further studies have shown that such a flatness is only approximate: brighter galaxies tend to have slightly falling rotation curves, whereas fainter ones possess slightly rising rotation curves [38]. Still, what really matters for the visible-invisible conspiracy (as stated above) is the lack of any jump in the rotation curve within the disk-halo transition region, besides the approximate flatness.

A priori, only a mysterious fine-tuning could justify the conspiracy in question if the halo dark matter were different in nature from luminous matter, that is to say if it were nonbaryonic. So, baryonic dark matter looks like a natural constituent of galactic halos. Incidentally, this situation is very reminiscent of the case of grand unified theories in particle physics, where supersymmetry has been invoked as a successful way out of a similar, mysterious fine-tuning needed to stabilize the gauge hierarchy against radiative corrections [39]. Thus, we are led to the conclusion that – much in the same way as fundamental interactions ought to be supersymmetric – galactic halos ought to be predominantly baryonic!

Remarkably enough, a specific model of baryonic dark halos emerges naturally from the present-day understanding of globular clusters. Indeed, a few years ago we have realized [28, 29] that the Fall-Rees theory for the formation of globular clusters [40]-[42] automatically predicts – without any further physical assumption – that dark clusters made of brown dwarfs † and cold H_2 clouds should lurk in the galactic halo at

† Although we concentrate our attention on brown dwarfs, it should be mentioned that red dwarfs as

galactocentric distances larger than 10–20 kpc. Accordingly, the inner halo is populated by globular clusters, whereas the outer halo chiefly consists of dark clusters. ‡ Below, we summarize the main features of our model.

Although the mechanism of galaxy formation is not yet fully understood, the theory for the origin of globular clusters seems to be fairly well established - thanks to the pioneering work of Fall and Rees [40] - and can be summarized as follows. After its initial collapse, the proto-galaxy is expected to be shock heated up to its virial temperature $\sim 10^6$ K. Because of thermal instability, density enhancements rapidly grow as the gas cools. Actually, overdense regions cool more rapidly than average, and so proto-globular-cluster (PGC) clouds form in pressure equilibrium with the hot diffuse gas. When the PGC cloud temperature drops to $\sim 10^4$ K, hydrogen recombination occurs: at this stage, the PGC cloud mass and size are $\sim 10^5(R/\text{kpc})^{1/2} M_\odot$ and $\sim 10(R/\text{kpc})^{1/2}$ pc, respectively (R being the galactocentric distance). Below $\sim 10^4$ K, an efficient cooling can be brought about only by photon emission from roto-vibrational transitions in H_2 . Whether this mechanism is actually operative or not crucially depends on the intensity of the environmental ultraviolet (UV) radiation field, as we are now going to discuss.

In fact, in the central region of the proto-galaxy an AGN (Active Galactic Nucleus) along with a first population of massive stars are expected to form, which act as strong sources of UV radiation that dissociates the H_2 molecules. It is not difficult to estimate that the H_2 destruction should occur for galactocentric distances smaller than 10 – 20 kpc. As a consequence, cooling is heavily suppressed in the inner halo, and so here the PGC clouds remain for a long time in quasi-hydrostatic equilibrium at temperature $\sim 10^4$ K, resulting in the imprinting of a characteristic mass $\sim 10^6 M_\odot$. Eventually, the UV flux decreases, thereby allowing for the formation and survival of H_2 . Accordingly, the PGC clouds can further cool, collapse and fragment, ultimately producing ordinary stars clumped into globular clusters.

What is most relevant for the present considerations is that in the outer halo – namely for galactocentric distances larger than 10 – 20 kpc – no substantial H_2 destruction should take place, owing to the distance suppression of the UV flux. Therefore, here the PGC clouds monotonically cool, collapse and fragment. When their number density exceeds $\sim 10^8 \text{ cm}^{-3}$, virtually all hydrogen gets converted to molecular form by three-body reactions ($H + H + H \rightarrow H_2 + H$ and $H + H + H_2 \rightarrow H_2 + H_2$), which makes in turn the cooling efficiency increase dramatically [54]. As a result, no imprinting of a characteristic mass on the PGC clouds shows up, and the fragment

well can be accommodated within the considered setting.

‡ Similar ideas have been proposed by Ashman and Carr [43], Ashman [44], Fabian and Nulsen [45, 46], and Kerins [47, 48]. Moreover, a scenario almost identical to the one investigated here has been put forward by Gerhard and Silk [49]. Somewhat different baryonic pictures have been worked out by Pfenniger, Combes and Martinet [50], Sciamia [51], and Gibson and Schild [52] (see also [53]).

Jeans mass can drop to values considerably smaller than $\sim 1M_{\odot}$. The fragmentation process stops when the PGC clouds become optically thick to their own line emission – this happens for a fragment Jeans mass as low as $\sim 10^{-2}M_{\odot}$ [54]. In this manner, dark clusters containing brown dwarfs in the mass range $10^{-2} - 10^{-1} M_{\odot}$ should form in the outer halo. Typical values of the dark cluster radius are ~ 10 pc.

In spite of the fact that the dark clusters resemble in many respects globular clusters, an important difference exists. Since practically no nuclear reactions occur in the brown dwarfs, strong stellar winds are presently lacking. Therefore the leftover gas - which is ordinarily expected to exceed 60% of the original amount - is not expelled from the dark clusters but remains confined inside them. Thus, also cold gas clouds are clumped into the dark clusters. Although these clouds are primarily made of H_2 , they should be surrounded by an atomic layer and a photo-ionized “skin”. Typical values of the cloud radius are $\sim 10^{-5}$ pc.

Besides accounting for the halo dark matter in a natural fashion - without demanding any new physical assumption - this model elegantly explains the visible-invisible conspiracy. For, whether ordinary matter is luminous or dark ultimately depends on the intensity of the environmental UV radiation field during the proto-galactic epoch - no fine-tuning is indeed involved! Moreover, the UV field in question is expected to be stronger for brighter galaxies. Accordingly, brighter galaxies should have the dark clusters lying farther away from the galactic centre than fainter galaxies, thereby making the contribution of dark matter to the rotation curve of brighter galaxies less significant than for fainter ones: this circumstance precisely agrees with the above-mentioned observed pattern of rotation curves [38].

Observationally, the present model makes a crucial prediction: very high-energy cosmic ray proton scattering on the clouds should give rise to a detectable diffuse gamma-ray flux from the halo of our galaxy. This topic will be dealt with in great detail in the next Sections.

Further support in favour of the baryonic scenario in question comes from the understanding of the Extreme Scattering Events: dramatic flux changes over several weeks during monitoring of compact radio quasars [55]. It is generally agreed that ESEs are not intrinsic variations, but rather apparent flux changes caused by refraction when a (partially) ionized cloud crosses the line of sight. Recently, Walker and Wardle [56] pointed out that the first consistent explanation of ESEs requires the refracting clouds to have precisely the same properties of the cold H_2 clouds predicted by the present model (it is their photo-ionized “skin” that causes the radio wave refraction).

Last but not least is the issue of MACHOs (Massive Astrophysical Compact Halo Objects), detected since 1993 in microlensing experiments towards the Magellanic Clouds. Regretfully, their origin remains controversial. Although the events detected towards the SMC (Small Magellanic Cloud) seem to be a self-lensing phenomenon

[57, 58], a similar interpretation of all the events discovered towards the LMC (Large Magellanic Cloud) looks unlikely [59]. Yet – even if most of the MACHOs are dark matter candidates lying in the galactic halo – their physical nature is unclear, since their average mass strongly depends on the still uncertain galactic model, ranging from $\sim 0.1 M_{\odot}$ for a maximal disk up to $\sim 0.5 M_{\odot}$ for a standard isothermal sphere.

Superficially, white dwarfs look as the best explanation, but the resulting excessive metallicity of the halo makes this option untenable, unless their contribution to halo dark matter is not substantial (see [60, 61]). So, some variations on the theme of brown dwarfs have been explored.

An option is that the galactic halo resembles more closely a minimal halo (maximal disk) rather than an isothermal sphere, in which case MACHOs can still be brown dwarfs. † In this connection, two points should be stressed. First, a large fraction (up to 50% in mass) can be binary systems - much like ordinary stars - thereby counting as twice more massive objects [63]. Second, within our model brown dwarfs can actually be beige dwarfs - with mass substantially larger than $\simeq 0.1 M_{\odot}$ - as suggested by Hansen [64], since a slow accretion mechanism from cloud gas is likely to occur [65].

An alternative possibility has been pointed out by Kerins and Evans [66]. Since in the present model the initial mass function obviously changes with the galactocentric distance, ‡ it can well happen that brown dwarfs dominate the halo mass density without however dominating the optical depth for microlensing. What are then MACHOs? Quite recently, faint blue objects discovered by the Hubble Space Telescope have been understood as old halo white dwarfs lying closer than ~ 2 kpc from the Sun [68]-[70]: they look as a good candidate for MACHOs within this context.

Finally, we remark that recently ISO observations [71] of the nearby NGC891 galaxy have detected a huge amount of molecular hydrogen, which might account for almost all dark matter, at least within its optical radius. Other observations suggest that similar clouds are also present farther away [72]. In addition, Sciama [51] has argued that a known excess in the far-infrared emissivity of our galaxy (over that expected from a standard warm interstellar dust model) would be naturally accounted for by a population of cold H_2 clouds building up a thick galactic disk.

3. Cosmic ray confinement in the galactic halo

Neither theory nor observation allow at present to make sharp statements about the propagation of CRs in the galactic halo §. Therefore, the only possibility to get

† Notice that also the H_2 clouds can give rise to microlensing events [62].

‡ Evidence for a spatially varying initial mass function in the galactic disk has been reported [67].

§ We stress that - contrary to the practice used in the CR community - by halo we mean the (almost) spherical galactic component which extends beyond ~ 10 kpc.

some insight into this issue rests upon the extrapolation from the knowledge of CR propagation in the disk. Actually, this strategy looks sensible, since the leading effect is CR scattering on inhomogeneities of the magnetic field over scales from 10^2 pc down to less than 10^{-6} pc [73] and - according to our model - inhomogeneities of this kind are expected to be present in the halo as well, because of the existence of molecular clouds - with a photo-ionized “skin” - clumped into dark clusters. Indeed, typical values of the dark cluster radius are ~ 10 pc, whereas typical values of the cloud radius are $\sim 10^{-5}$ pc [32].

As is well known, CRs up to energies of $\sim 10^6$ GeV are confined in the galactic disk for $\sim 10^7$ yr [73]. It can be shown that in the diffusion model for the propagation of CRs, the escape time τ_{esc} is given by [73]

$$\tau_{esc} \simeq \frac{R_h^2}{3D(E)} \frac{1 - \frac{1}{2} \left(\frac{h_d}{R_h}\right)^2 + \frac{1}{8} \left(\frac{h_d}{R_h}\right)^3}{1 - \frac{h_d}{2R_h}}, \quad (4)$$

where $D(E)$ is the diffusion coefficient, while h_d and R_h are the half-thickness of the disk and the radius of the confinement region, respectively. We remind that - for CR propagation in the disk - the diffusion coefficient is $D(E) \simeq D_0 (E/7 \text{ GeV})^{0.3} \text{ cm}^2 \text{ s}^{-1}$ in the ultra-relativistic regime, whereas it reads $D(E) \simeq D_0 \simeq 3 \times 10^{28} \text{ cm}^2 \text{ s}^{-1}$ in the non-relativistic regime [73].

CRs escaping from the disk will further diffuse in the galactic halo, where they can be retained for a long time, owing to the scattering on the above-mentioned small inhomogeneities of the halo magnetic field †.

Indirect evidence that CRs are in fact trapped in a low-density halo has recently been reported. For example, Simpson & Connell [75] argue that, based on measurements of isotopic abundances of the cosmic ratio $^{26}\text{Al}/^{27}\text{Al}$, the CR lifetimes are perhaps a factor of four larger than previously thought, thereby implying that CRs traverse an average density smaller than that of the galactic disk.

A straightforward extension of the diffusion model implies that the CR escape time τ_{esc}^H from the halo (of size $R_H \equiv R_h \sim 100$ kpc, much larger than the disk half-thickness) is given by

$$\tau_{esc}^H \simeq \frac{R_H^2}{3D_H(E)}, \quad (5)$$

where $D_H(E)$ is the diffusion coefficient in the galactic halo.

As a matter of fact, radio observations in clusters of galaxies yield for the corresponding diffusion constant D_0 a value similar to that found in the galactic disk

† A similar idea has been proposed with a somewhat different motivation in [74].

[76] ‡. So, it looks plausible that a similar value for D_0 also holds on intermediate length scales, namely within the galactic halo. In the lack of any further information on the energy-dependence of $D_H(E)$, we assume the same dependence as that established for the disk. Hence, from eq. (5) we find that for energies $E \lesssim 10^3$ GeV the escape time of CRs from the halo is greater than the age of the Galaxy $t_0 \simeq 10^{10}$ yr (notice that below the ultra-relativistic regime τ_{esc}^H gets even longer). As a consequence - since the CR flux scales like $E^{-2.7}$ (see next Section) - protons with $E \lesssim 10^3$ GeV turn out to give the leading contribution to the CR flux.

We are now in position to evaluate the CR energy density in the galactic halo, getting

$$\rho_{CR}^H \simeq \frac{3t_0 L_G}{4\pi R_H^3} \simeq 0.12 \quad \text{eV cm}^{-3}, \quad (6)$$

where $L_G \simeq 10^{41}$ erg s⁻¹ is the galactic CR luminosity (see, e.g., [78]). Notice, for comparison, that ρ_{CR}^H turns out to be about one-tenth of the disk value [79]. In fact, this value is consistent with the EGRET upper bound on the CR density in the halo near the SMC [80].

We remark that we have taken specific realistic values for the various parameters entering the above equations in order to make a quantitative estimate. However, somewhat different values can be used. For instance, R_H may range up to ~ 200 kpc [34], whereas D_0 might be slightly larger than the above value, e.g. $\simeq 10^{29}$ cm² s⁻¹ consistently with our assumptions. Moreover, L_G can be as large as 3×10^{41} erg s⁻¹ [81]. It is easy to see that these variations do not substantially affect our previous conclusions.

4. Proton-proton scattering in the galactic halo

We proceed to estimate the halo γ -ray flux produced by the clouds clumped into dark clusters through the interaction with high-energy CR protons. CR protons scatter on cloud protons giving rise (in particular) to neutral pions, which subsequently decay into photons. A highly nontrivial question concerns the opacity effects in the clouds. Quite recently, Kalberla et al. [82] have addressed precisely this issue, showing that optical-depth effects for both protons and photons are negligible within our model. Finally, we expect an irrelevant high-energy (≥ 100 MeV) γ -ray photon absorption outside the clouds, since the mean free path is orders of magnitudes larger than the halo size.

As far as the energy-dependence of the halo CRs is concerned, we adopt the same

‡ Moreover, we note that average magnetic field values in galactic halos are expected to be close to those of galaxy clusters, i.e. between $0.1 \mu\text{G}$ and $1 \mu\text{G}$ [77].

power-law as in the galactic disk (see below) [79]

$$\Phi_{CR}^H(E) \simeq \frac{A}{\text{GeV}} \left(\frac{E}{\text{GeV}} \right)^{-\alpha} \text{ particles cm}^{-2} \text{ s}^{-1} \text{ sr}^{-1}. \quad (7)$$

The constant A is fixed by the requirement that the integrated energy flux agrees with the above value of ρ_{CR}^H . Explicitly

$$\int d\Omega dE E \Phi_{CR}^H(E) \simeq 5.7 \times 10^{-3} \text{ erg cm}^{-2} \text{ s}^{-1}, \quad (8)$$

where for definiteness we take the integration range to be $1 \text{ GeV} \leq E \leq 10^3 \text{ GeV}$. A nontrivial point concerns the choice of α . As an orientation, the observed spectrum of primary CRs on Earth would yield $\alpha \simeq 2.7$. However, this conclusion cannot be extrapolated to an arbitrary region in the halo (and in the disk), since α crucially depends on the diffusion processes undergone by CRs. For instance, the best fit to EGRET data in the disk towards the galactic centre yields $\alpha \simeq 2.45$ [83], thereby showing that α gets increased by diffusion. In the lack of any direct information, we conservatively take $\alpha \simeq 2.7$ even in the halo, but in Table 1 we report some results for different values of α for comparison. At any rate, the flux does not vary substantially.

Table 1. Halo γ -ray intensity at high-galactic latitude for a spherical halo evaluated for $R_{min} = 10$ and 15 kpc at energies above 0.1 GeV and 1 GeV, for different values of the CR spectral index α is given in units of $10^{-7} \gamma \text{ cm}^{-2} \text{ s}^{-1} \text{ sr}^{-1}$.

R_{min} (kpc)	E_γ (GeV)	α	$\Phi_\gamma^{\text{DM}}(b = 90^\circ)$
10	> 0.1	2.45	62
		2.70	59
		3.00	49
10	> 1.0	2.45	11
		2.70	6.7
		3.00	3.3
15	> 0.1	2.45	37
		2.70	35
		3.00	29
15	> 1.0	2.45	6.5
		2.70	4.0
		3.00	1.9

Let us next turn our attention to the evaluation of the γ -ray flux produced in halo clouds through the reactions $pp \rightarrow \pi^0 \rightarrow \gamma\gamma$. Accordingly, the source function

$q_\gamma(> E_\gamma, \rho, l, b)$ - yielding the photon number density at distance ρ from Earth with energy greater than E_γ - is [79]

$$q_\gamma(> E_\gamma, \rho, l, b) = \frac{4\pi}{m_p} \rho_{H_2}(\rho, l, b) \times \sum_n \int_{E_p(E_\gamma)}^\infty dE_p dE_\pi \Phi_{CR}^H(E_p) \frac{d\sigma_{p \rightarrow \pi}^n(E_\pi)}{dE_\pi} n_\gamma(E_p) , \quad (9)$$

where the lower integration limit $E_p(E_\gamma)$ is the minimal proton energy necessary to produce a photon with energy $> E_\gamma$, $\sigma_{p \rightarrow \pi}^n(E_\pi)$ is the cross-section for the reaction $pp \rightarrow n\pi^0$ (n is the π^0 multiplicity), $\rho_{H_2}(\rho, l, b)$ is the halo gas density profile and $n_\gamma(E_p)$ is the photon multiplicity.

Unfortunately, it would be exceedingly difficult to keep track of the clumpiness of the actual gas distribution in the halo, and so we assume that its density is smooth and goes like the dark matter density - anyhow, the very low angular resolution of γ -ray detectors would not permit to distinguish between the two situations (evidently this strategy would be meaningless if optical-depth effects were not negligible). Accordingly, the halo gas density profile reads

$$\rho_{H_2}(x, y, z) = f \rho_0(q) \frac{\tilde{a}^2 + R_0^2}{\tilde{a}^2 + x^2 + y^2 + (z/q)^2} , \quad (10)$$

for $\sqrt{x^2 + y^2 + z^2/q^2} > R_{min}$, ($R_{min} \simeq 10$ kpc is the minimal galactocentric distance of the dark clusters in the galactic halo). We recall that f denotes the fraction of halo dark matter in the form of gas, $\rho_0(q)$ is the local dark matter density, $\tilde{a} = 5.6$ kpc is the core radius and q measures the halo flattening. For the standard spherical halo model $\rho_0(q = 1) \simeq 0.3$ GeV cm⁻³, whereas it turns out that e.g. $\rho_0(q = 0.5) \simeq 0.6$ GeV cm⁻³.

In order to proceed further, it is convenient to re-express $q_\gamma(> E_\gamma, \rho, l, b)$ in terms of the inelastic pion production cross-section $\sigma_{in}(p_{lab})$. Since

$$\sigma_{in}(p_{lab}) < n_\gamma(E_p) > = \sum_n \int dE_\pi \frac{d\sigma_{p \rightarrow \pi}^n(E_\pi)}{dE_\pi} n_\gamma(E_p) , \quad (11)$$

eq. (9) becomes

$$q_\gamma(> E_\gamma, \rho, l, b) = \frac{4\pi}{m_p} \rho_{H_2}(\rho, l, b) \times \int_{E_p(E_\gamma)}^\infty dE_p \Phi_{CR}^H(E_p) \sigma_{in}(p_{lab}) < n_\gamma(E_p) > , \quad (12)$$

where $\rho_{H_2}(\rho, l, b)$ is given by eq. (10) with $x = -\rho \cos b \cos l + R_0$, $y = -\rho \cos b \sin l$ and $z = \rho \sin b$.

For the inclusive cross-section of the reaction $pp \rightarrow \pi^0 \rightarrow \gamma\gamma$ we adopt the Dermer

[84] parameterization

$$\sigma_{in}(p) < n_\gamma(E_p) > = 2 \times 1.45 \times 10^{-27} \times \begin{cases} 0.032\eta^2 + 0.040\eta^6 + 0.047\eta^8 & 0.78 \leq p \leq 0.96 \\ 32.6(p - 0.8)^{3.21} & 0.96 \leq p \leq 1.27 \\ 5.40(p - 0.8)^{0.81} & 1.27 \leq p \leq 8.0 \\ 32\ln p + 48.5p^{-1/2} - 59.5 & p \geq 8.0 , \end{cases} \quad (13)$$

where p is the proton laboratory momentum in GeV/c, the factor 2 comes from the fact that each pion decays into two photons, whereas 1.45 accounts for the CR composition [84], which includes also heavy nuclei. The quantity

$$\eta \equiv \frac{[(s - m_\pi^2 - m_p^2)^2 - 4m_\pi^2 m_p^2]^{1/2}}{2m_\pi s^{1/2}} , \quad (14)$$

is expressed in terms of the Mandelstam variable s , while m_π and m_p are the pion and the proton mass, respectively.

Because $dV = \rho^2 d\rho d\Omega$, it follows that the observed γ -ray flux per unit solid angle is

$$\Phi_\gamma^{\text{DM}}(> E_\gamma, l, b) = \frac{1}{4\pi} \int_{\rho_1(l,b)}^{\rho_2(l,b)} d\rho q_\gamma(> E_\gamma, \rho, l, b) . \quad (15)$$

So, we find

$$\Phi_\gamma^{\text{DM}}(> E_\gamma, l, b) = f \frac{\rho_0(q)}{m_p} I_1(l, b) I_2(> E_\gamma) , \quad (16)$$

where $I_1(l, b)$ and $I_2(> E_\gamma)$ are defined as

$$I_1(l, b) \equiv \int_{\rho_1(l,b)}^{\rho_2(l,b)} d\rho \left(\frac{\tilde{a}^2 + R_0^2}{\tilde{a}^2 + x^2 + y^2 + (z/q)^2} \right) , \quad (17)$$

$$I_2(> E_\gamma) \equiv \int_{E_p(E_\gamma)}^\infty dE_p \Phi_{CR}^H(E_p) \sigma_{in}(p_{lab}) < n_\gamma(E_p) > , \quad (18)$$

and m_p is the proton mass.

According to the discussion in Sections 2 and 3, typical values of $\rho_1(l, b)$ and $\rho_2(l, b)$ in eqs. (15) and (17) are 10 kpc and 100 kpc, respectively. Numerical values for Φ_γ^{DM} in the cases $\alpha = 2.45, 2.7$ and 3.0 are reported in Table 1.

5. Inverse-Compton scattering

Another mechanism whereby γ -ray photons are produced is IC scattering of high-energy CR electrons off galactic background photons. Here we estimate the resulting flux, while the interplay between proton-proton scattering and IC scattering will be discussed in the next Section.

The electron injection spectrum which best fits the locally observed electron spectrum is given by the following power-law valid for $E_e \gtrsim 10$ GeV (see e.g. [85])

$$I_e(E_e; \rho, l, b) = K(\rho, l, b) E_e^{-a} \text{ e}^- \text{ cm}^{-2} \text{ s}^{-1} \text{ sr}^{-1} \text{ GeV}^{-1}, \quad (19)$$

with $a \simeq 2.4$ and $K_0 \equiv K(0) \simeq 6.3 \times 10^{-3} \text{ e}^- \text{ cm}^{-2} \text{ s}^{-1} \text{ sr}^{-1} \text{ GeV}^{a-1}$ (the value of K_0 is obtained by normalizing eq. (19) with the observed local CR electron spectrum at 10 GeV). Since a is somewhat model-dependent (in particular it depends on the diffusion processes), its actual value is not well determined, and indeed it could be as low as $a \simeq 2$ [4] or even $a \simeq 1.8$ [5]. However, what is relevant is the electron spectrum where the γ -ray production occurs and - due to diffusion processes - the value of a is expected to increase with the distance from the galactic plane where the electrons are mostly produced.

In order to estimate the galactic radiation field, we adopt the model of Mazzei, Xu & De Zotti [86] for the photometric evolution of disk galaxies. This model reproduces well the present broad-band spectrum of the Galaxy over about four decades in frequency, from UV to far-IR. Accordingly, the two main contributions to the galactic radiation field come from stars at wavelength $\lambda \sim 1\mu\text{m}$ and diffuse dust at $\lambda \sim 100\mu\text{m}$. The total stellar luminosity of the Galaxy is $L_\star \sim 3.5 \times 10^{10} L_\odot$ and the amount of starlight absorbed and re-emitted by dust is $L_d \sim 1.2 \times 10^{10} L_\odot$ (see e.g., [86, 87]). As regards to the photon energy distribution, we can roughly approximate the emission spectrum (see Fig. 4 in [86]) with the sum of two Planck functions with temperature $T_\star \sim 2900$ K and $T_d \sim 29$ K, respectively.

According to the previous assumptions, the source function $q_{\text{ph}}(E_\gamma)$ for γ -ray production through IC scattering is given by [73]

$$q_{\text{ph}}(E_\gamma) = \frac{1}{2} \sigma_T \left(\frac{4}{3} \langle \epsilon_{\text{ph}}(T_{\star,d}) \rangle \right)^{(a-1)/2} \times \quad (20)$$

$$(mc^2)^{1-a} K_0 E_\gamma^{-(a+1)/2} \text{ } \gamma \text{ s}^{-1} \text{ sr}^{-1} \text{ GeV}^{-1}.$$

Here $\langle \epsilon_{\text{ph}}(T_{\star,d}) \rangle \simeq 8kT_{\star,d}/3$ is the average energy of background photons emitted by stars or dust and σ_T is the Thompson cross-section. In deriving eq. (20), use is made of the fact that the γ -ray energy is related to the electron and background photon energies according to

$$\langle E_\gamma \rangle = \frac{4}{3} \langle \epsilon_{\text{ph}}(T_{\star,d}) \rangle \left(\frac{E_e}{mc^2} \right)^2, \quad (21)$$

so that very high-energy electrons are needed in order to produce γ -rays. For example, a γ -ray with $E_\gamma \simeq 1$ GeV produced by this mechanism requires $E_e \simeq 170$ GeV for a target photon emitted by dust, while $E_e \simeq 17$ GeV is demanded for starlight.

The intensity of diffuse galactic γ -rays of energy $> E_\gamma$ produced in this way and

coming to Earth along the line-of-sight (l, b) turns out to be

$$\begin{aligned} \Phi_{\gamma}^{\text{IC}}(> E_{\gamma}, l, b) &= \int_0^{\infty} d\rho \langle n_{\text{ph}}(\rho, l, b) \rangle f_e(\rho, l, b) \times \\ &\int_{E_{\gamma}}^{\infty} q_{\text{ph}}(E_{\gamma}) dE_{\gamma} \quad \gamma \text{ cm}^{-2} \text{ s}^{-1} \text{ sr}^{-1}, \end{aligned} \quad (22)$$

where we have introduced the function $f_e(\rho, l, b) \equiv K(\rho, l, b)/K_0$ as the ratio of the electron CR intensity relative to the local intensity, while $\langle n_{\text{ph}}(\rho, l, b) \rangle$ is the average density of background photons.

Let us next focus our attention on the functions $f_e(\rho, l, b)$ and $\langle n_{\text{ph}}(\rho, l, b) \rangle$. The electron component of CRs is galactic in origin, mainly produced by supernovae and pulsars located inside the disk. Electrons diffuse through the Galaxy and their distribution is energy-dependent and not uniform, namely, the characteristic diffusion length scale gets smaller for higher electron energy. This feature cannot be described in the framework of the widely used Leaky Box Model, and in order to obtain the electron density at an arbitrary point in the Galaxy one has to resort to the transport equation (see e.g. [4, 73]). Unfortunately, several fairly unknown parameters enter this equation, like the electron diffusion coefficient, the rate at which electrons lose energy, the density of sources and the electron spectrum.

An alternative approach relies upon the experimental evidence of the thick disk †, in which high-energy electrons may be retained for a long time before escaping into the galactic halo. Indeed, the observed characteristics of the radio emission spectra of our and other galaxies lead to a relative density distribution of electrons $f_e(R_0, z) \equiv n_e(z)/n_e(0)$ extending up to 5 – 12 kpc perpendicularly to the galactic plane, as shown in Figure 5.29 of [73]. These numerical results can be approximated by $f_e(R_0, z) = \exp[-(z/z_e)^{3/2}]$, with the parameter z_e depending on the electron energy. From eq. (21) and the ensuing discussion, it turns out that $z_e \simeq 2.5$ kpc for $E_e \simeq 170$ GeV while $z_e \simeq 3.5$ kpc for $E_e \simeq 17$ GeV. As far as the radial dependence of the electron distribution is concerned, we assume that $f_e(R, 0)$ follows the same R -dependance of the CRs, which can be obtained by using a best fit procedure to the data in Figure 11 of [88]. This yields

$$f_e(R, 0) = e^{[0.48 - 0.36(R/R_0) - 0.12(R/R_0)^2]}. \quad (23)$$

However, following Bloemen [88] - who suggested a stronger radial gradient for the electron component of the CRs - we also tested the effect of using a steeper radial electron distribution on the IC γ -ray flux. We anticipate that the corresponding results show that the IC γ -ray flux does not change significantly for galactic longitudes $|l| \leq 90^\circ$ (irrespectively of the latitude values) while it increases up to a factor of two at $l = 180^\circ$ for $|b| \leq 30^\circ$.

† Often defined as “halo” by the CR community.

The last quantity to be specified in eq. (22) is the average background photon density $\langle n_{ph}(\rho, l, b) \rangle$ or, equivalently, the background photon flux $\Phi_{ph}(\rho, l, b)$ emitted by stars and dust

$$\langle n_{ph}(\rho, l, b) \rangle = \frac{\Phi_{ph}(\rho, l, b)}{c} \quad \gamma \text{ cm}^{-3} . \quad (24)$$

Note that the photon flux $d\Phi_{ph}(\rho, l, b)$ at a point $P(\rho, l, b)$ from the solid angle $d\Omega$ subtended by an infinitesimal area da' centered in $P'(R', \phi', z' = 0)$ on the galactic plane is given by

$$d\Phi_{ph}(\rho, l, b) = I_{*,d}(R') \left(\frac{d\Omega}{4\pi} \right) \cos \alpha \quad \gamma \text{ cm}^{-2} \text{ s}^{-1} , \quad (25)$$

where α is the angle between the normal to the area da' and the direction \mathbf{PP}' . We can trace the surface brightness $I_{*,d}(R')$ to the stellar/dust distribution. Assuming that visible matter makes up an exponential disk, we set

$$I_{*,d}(R') = A_{*,d} e^{-(R'-R_0)/h_{*,d}} \quad \gamma \text{ cm}^{-2} \text{ s}^{-1} , \quad (26)$$

where $h_{*,d} \simeq 3.5$ kpc is the scale length for the visible matter and the constant $A_{*,d}$ is fixed by the total disk luminosity as

$$\int_0^{R_d} I_{*,d}(R') 2\pi R' dR' = \frac{L_{*,d}}{2 \langle \epsilon_{ph}(T_{*,d}) \rangle} \quad \gamma \text{ s}^{-1} . \quad (27)$$

In this way, we get $A_* = 4.71 \times 10^{20} \gamma \text{ cm}^{-2} \text{ s}^{-1}$ and $A_d = 1.64 \times 10^{22} \gamma \text{ cm}^{-2} \text{ s}^{-1}$, with $R_d \simeq 15$ kpc. By integrating eq. (25) on the galactic disk, we find

$$\Phi_{ph}(\rho, l, b) = \int_0^{R_d} \int_0^{2\pi} I_{*,d}(R') R' dR' d\phi' \left(\frac{\cos \alpha}{4\pi |\mathbf{PP}'|^2} \right) \quad \gamma \text{ cm}^{-2} \text{ s}^{-1} . \quad (28)$$

Finally, by using eqs. (24), (26) and (28) - and recalling eq. (20) - eq. (22) can be rewritten in the form

$$\Phi_\gamma^{\text{IC}}(> E_\gamma, l, b) = J_1(l, b) J_2(> E_\gamma) \quad \gamma \text{ cm}^{-2} \text{ s}^{-1} \text{ sr}^{-1} , \quad (29)$$

where we have set

$$J_1(l, b) \equiv \int_0^\infty f_e(\rho, l, b) d\rho \times \int_0^{R_d} \int_0^{2\pi} \left(\frac{\cos \alpha}{4\pi |\mathbf{PP}'|^2} \right) R' dR' d\phi' e^{-(R'-R_0)/h_{*,d}} \quad \text{cm} , \quad (30)$$

and

$$J_2(> E_\gamma) \equiv \frac{A_{*,d}}{2c} \sigma_T [4/3 \langle \epsilon_{ph}(T_{*,d}) \rangle]^{(a-1)/2} \times \quad (31)$$

$$(mc^2)^{1-a} K_0 \int_{E_\gamma}^\infty E_\gamma^{-(a+1)/2} dE_\gamma \quad \gamma \text{ cm}^{-3} \text{ s}^{-1} \text{ sr}^{-1} .$$

Numerical values of $\Phi_\gamma^{\text{IC}}(> E_\gamma, l, b)$ at high-galactic latitude are exhibited in Table 2 and plotted in Figure 3.

Table 2. The galactic diffuse γ -ray intensity due to IC scattering of high-energy electrons on background photons from stars and dust is given (in units of $10^{-7} \gamma \text{ cm}^{-2} \text{ s}^{-1} \text{ sr}^{-1}$) for $a = 2.0, 2.4$ and 2.8 . The results for $a = 2, 2.8$ are reported for illustrative purposes. We adopt the following values: $T_* = 2900 \text{ K}$, $L_* = 3.5 \times 10^{10} L_\odot$ and $T_d = 29 \text{ K}$, $L_d = 1.5 \times 10^{10} L_\odot$.

	z_e	E_γ	$\Phi_\gamma^{\text{IC}}(90^\circ)$	$\Phi_\gamma^{\text{IC}}(90^\circ)$	$\Phi_\gamma^{\text{IC}}(90^\circ)$
	(kpc)	(GeV)	$a = 2.0$	$a = 2.4$	$a = 2.8$
stars	3.5	> 0.1	3.8	3.5	3.4
		> 1.0	1.2	0.7	0.4
dust	2.5	> 0.1	12	4.4	1.7
		> 1.0	3.8	0.9	0.2

6. Discussion

Our main result are maps for the intensity distribution of the γ -ray emission from baryonic dark matter (DM) in the galactic halo and from IC processes in the galactic disk. In order to make the discussion definite, we take the fraction of halo dark matter in the form of molecular clouds $f \simeq 0.5$. As far as the IC emission is concerned, the standard electron spectral index $a = 2.4$ is used. We stress that the shape of the IC maps does not depend on the value of a .

In Figures 1 we exhibit the contour plots in the first quadrant of the sky ($0^\circ \leq l \leq 180^\circ$, $0^\circ \leq b \leq 90^\circ$) for the halo γ -ray flux $\Phi_\gamma^{\text{DM}}(E_\gamma > 1 \text{ GeV})$. Corresponding contour plots for $E_\gamma > 0.1 \text{ GeV}$ are identical, up to an overall constant factor equal to 8.74, as follows from eq. (16).

Figure 1a refers to a spherical halo, whereas Figure 1b pertains to a $q = 0.5$ flattened halo. Regardless of the adopted value for q , $\Phi_\gamma^{\text{DM}}(E_\gamma > 1 \text{ GeV})$ lies in the range $\simeq 6 - 8 \times 10^{-7} \gamma \text{ cm}^{-2} \text{ s}^{-1} \text{ sr}^{-1}$ at high-galactic latitude. However, the shape of the contour lines strongly depends on the flatness parameter. Indeed, for $q \gtrsim 0.9$ there are two contour lines (for each flux value) approximately symmetric with respect to $l = 90^\circ$ (see Figure 1a). On the other hand, for $q \lesssim 0.9$ there is a single contour line (for each value of the flux) which varies much less with the longitude (see Figure 1b).

As we can see from Table 1 and Figures 1, the predicted value for the halo γ -ray flux at high-galactic latitude is close to that found by Dixon et al. [1] (see also Table 3). This conclusion holds almost irrespectively of the flatness parameter.

Moreover, the comparison of the overall shape of the contour lines in our Figures 1a and 1b with the corresponding ones in Figure 3 of Ref. [1] entails that models with flatness parameter $q \lesssim 0.8$ are in better agreement with the data, thereby implying that

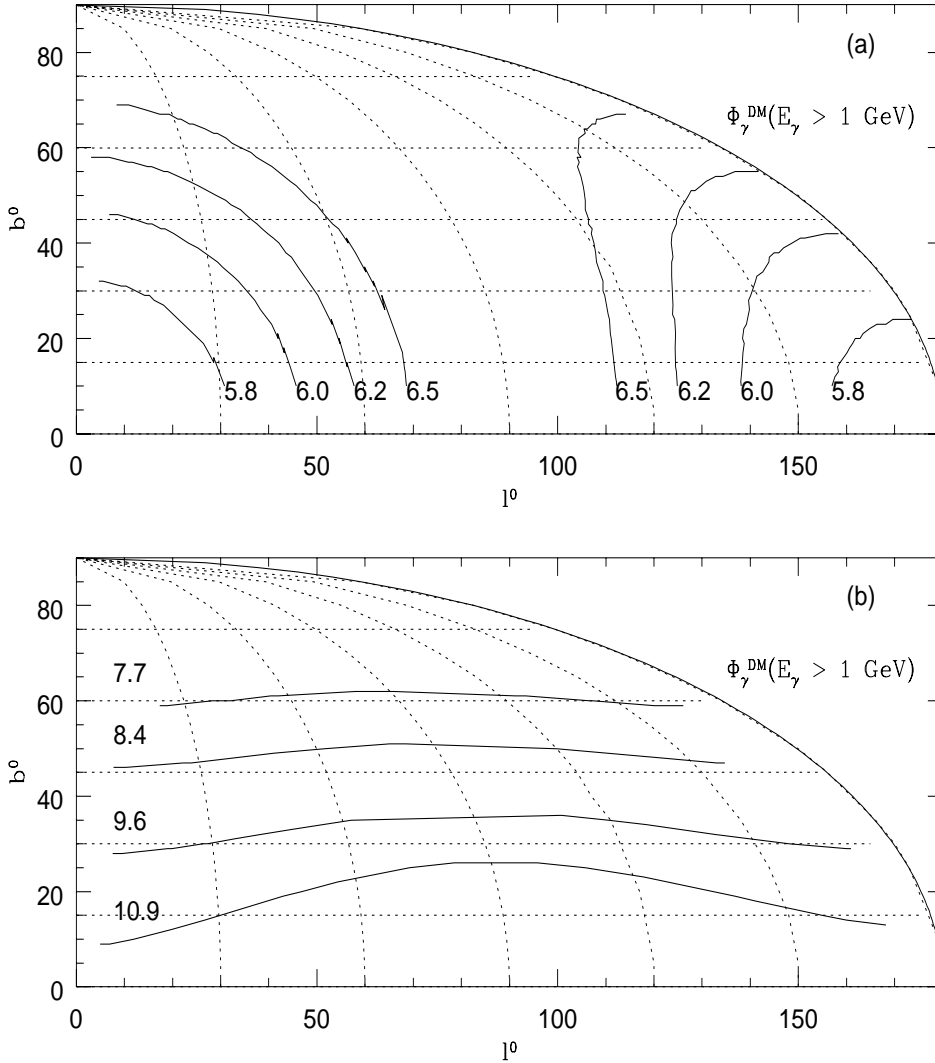


Figure 1. Contour values for the γ -ray flux due to the DM at $E_\gamma > 1 \text{ GeV}$ are given for the indicated values in units of $10^{-7} \text{ } \gamma \text{ cm}^{-2} \text{ s}^{-1} \text{ sr}^{-1}$, in the cases: (a) spherical halo, (b) flattened halo with $q = 0.5$.

most likely the halo dark matter is not spherically distributed. This result has been also recently confirmed in the analysis by [82].

In Figure 2 we present contour plots for the γ -ray flux due to the IC scattering, for $E_\gamma > 1 \text{ GeV}$. The corresponding contour plots for $E_\gamma > 0.1 \text{ GeV}$ are identical, up to an overall constant factor equal to 5 (this follows from eq. (31)). The contour lines decrease with increasing longitude.

We remark that eq. (16) yields $\Phi_\gamma^{DM}(E_\gamma > 0.1 \text{ GeV}) \simeq 5.9 \times 10^{-6} \text{ } \gamma \text{ cm}^{-2} \text{ s}^{-1} \text{ sr}^{-1}$ at high-galactic latitude (for a spherical halo). This value is roughly 40% of the diffuse

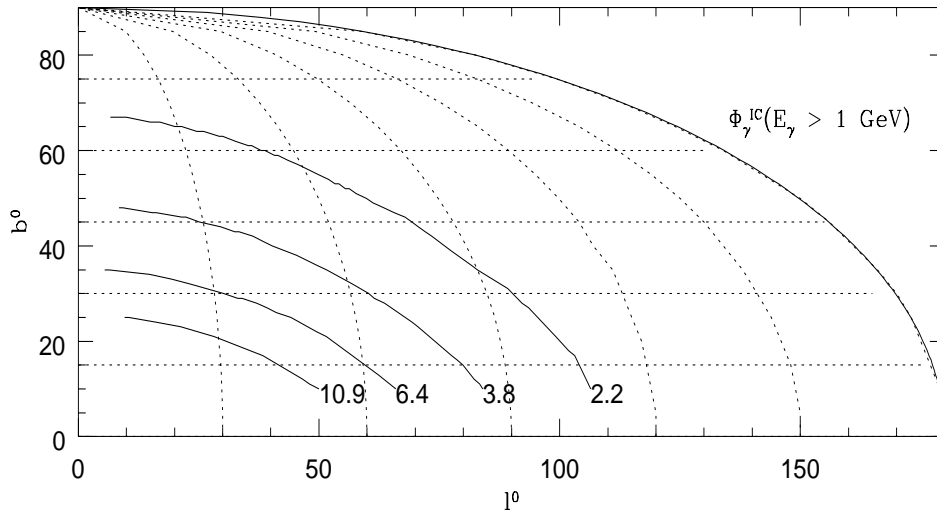


Figure 2. Contour values for the γ -ray flux due to the IC at $E_\gamma > 1$ GeV are given for the indicated values in units of $10^{-7} \gamma \text{ cm}^{-2} \text{ s}^{-1} \text{ sr}^{-1}$.

γ -ray emission of $(1.45 \pm 0.05) \times 10^{-5} \gamma \text{ cm}^{-2} \text{ s}^{-1} \text{ sr}^{-1}$ found by the EGRET team [6] and in agreement with the conclusion of Dixon et al. [1] that the halo γ -ray emission is a relevant fraction of the standard isotropic diffuse flux also for $E_\gamma > 0.1$ GeV.

Table 3. Rough values of the measured residual γ -ray flux at $E_\gamma \geq 1$ GeV (after subtraction of both the isotropic background and the standard galactic diffuse component) is given for different galactic latitude and longitude values (interpolated from Fig. 3a in [1]). Fluxes are given in units of $10^{-6} \gamma \text{ cm}^{-2} \text{ s}^{-1} \text{ sr}^{-1}$.

b	$l = 0^0$	$l = 60^0$
45^0	1	1
30^0	2	1.5
15^0	5.5	2

Nevertheless, given the large uncertainties both in the data and in the model parameters (such as for instance the electron scale height and the electron spectral index a), one might also explain the observations with a nonstandard IC mechanism [5]. Our calculation, however, seems to point out that the IC contour lines in Figure 2 decrease much more rapidly than the observed ones for the halo γ -ray emission (see Figure 3 in [1]). More precise measurements with a next generation of satellites are certainly required in order to settle the issue.

7. Gamma rays from the halo of M31

As M31 resembles our galaxy, the discovery of Dixon et al. [1] naturally leads to the expectation that the halo of M31 should give rise to a γ -ray emission as well. Below, we will try to address this issue in a quantitative manner, assuming that the halo of M31 is structurally similar to that of our galaxy and that our model for baryonic dark matter is correct.

We suppose that the various parameters entering the calculations in Sections 3 and 4 take similar values for M31 and for the Galaxy, apart from the M31 central dark matter density $\rho(0) \simeq 2.5 \times 10^{-24} \text{ g cm}^{-3}$ and the M31 core radius $\tilde{a} \simeq 5 \text{ kpc}$. Accordingly, the evaluation of the corresponding flux $\Phi_{\gamma}^{M31}_{halo}$ proceeds as before, with only minor modifications. Specifically, we can use again eq. (16) - with I_2 still given by eq. (18) - but now I_1 is to be replaced by L_1 (see below), in order to account for the different geometry. Notice that f in eq. (16) presently denotes the fraction of halo dark matter of M31 in the form of H_2 clouds.

Consider a generic point P in the halo of M31, and let R and r denote its distance from the centre O of M31 and from Earth, respectively. Since the distance of O from Earth is $D \simeq 650 \text{ kpc}$, we have $R(r) = (r^2 + D^2 - 2rD\cos\theta)^{1/2}$, where θ is the angular separation between P and O as seen from Earth. For simplicity, we suppose that the M31 halo is described by an isothermal sphere with radius R_H and density profile

$$\rho(R) = \frac{\rho(0)}{1 + (R/\tilde{a})^2} . \quad (32)$$

Note that the ensuing amount of dark matter in M31 turns out to be about twice as large as that of the Galaxy.

According to the discussion in Section 2, the dark clusters should populate only the outer halo of M31. So, we compute $\Phi_{\gamma}^{M31}_{halo}$ from regions of the M31 halo with $R_{min} < R < R_H$, with $R_{min} \simeq 10 \text{ kpc}$ and $R_H \simeq 100 \text{ kpc}$, for definiteness. As it is easy to see, the values of θ corresponding to R_{min} and R_H are $\theta_{min} \simeq 1^\circ$ and $\theta_H \simeq 9^\circ$, respectively.

We are now in position to compute L_1 , which reads

$$L_1 = 2\pi \int_{\theta_{min}}^{\theta_H} \sin\theta \, d\theta \int_{r_{min}(\theta)}^{r_{max}(\theta)} dr \left(\frac{\tilde{a}^2}{\tilde{a}^2 + R^2(r)} \right) \simeq 1.9 \times 10^{20} \text{ cm sr} , \quad (33)$$

with $r_{max(min)}(\theta) \equiv D\cos\theta + (-)(R_H^2 - D^2\sin^2\theta)^{1/2}$. Recalling eqs. (16) and (18), we get

$$\Phi_{\gamma}^{M31}_{halo}(> E_{\gamma}) = 1.9 \times 10^{20} f \frac{\rho(0)}{m_p} I_2(> E_{\gamma}) \quad \gamma \text{ cm}^{-2} \text{ s}^{-1} . \quad (34)$$

Observe that regions of M31 halo with angular separation less than θ_{min} from O do not contribute in eqs. (33) and (34), and so $\Phi_{\gamma}^{M31}_{halo}$ should be regarded as a lower bound on the total γ -ray flux from M31 halo.

Specifically, eq. (34) yields

$$\Phi_{\gamma}^{M31\text{ halo}}(E_{\gamma} > 0.1 \text{ GeV}) \simeq 3.5 \times 10^{-7} f \quad \gamma \text{ cm}^{-2} \text{ s}^{-1} . \quad (35)$$

This value has to be compared both with the γ -ray flux from M31 disk and with the γ -ray emission from the halo of the Galaxy. The former quantity has been estimated to be $\simeq 0.2 \times 10^{-7} \gamma \text{ cm}^{-2} \text{ s}^{-1}$ for $E_{\gamma} > 0.1 \text{ GeV}$ [89, 90] within a field of view of $1.5^{\circ} \times 6^{\circ}$, whereas the latter quantity, integrated over the entire field of view of M31 halo, is $\simeq 4.3 \times 10^{-7} \gamma \text{ cm}^{-2} \text{ s}^{-1}$ for $E_{\gamma} > 0.1 \text{ GeV}$, according to our results in Section 4 and 6. †

As far as observation is concerned, no γ -ray flux from M31 has been detected by EGRET. Accordingly, the EGRET team has derived the upper bound [91]

$$\Phi_{\gamma}^{M31}(E_{\gamma} > 0.1 \text{ GeV}) \lesssim 0.8 \times 10^{-7} \quad \gamma \text{ cm}^{-2} \text{ s}^{-1} . \quad (36)$$

Unfortunately, a direct comparison between eqs. (35) and (36) is hindered by the fact that eq. (36) is derived under the assumption of a point-like source.

Clearly, a good angular resolution of about one degree or less is necessary in order to discriminate between the halo and disk emission from M31. So, the next generation of γ -ray satellites like AGILE and GLAST can test our predictions.

Acknowledgments

We would like to thank G. Bignami, P. Caraveo, D. Dixon, T. Gaisser, M. Gibilisco, G. Kanbach, T. Stanev, A. Strong and M. Tavani for useful discussions.

References

- [1] Dixon D D et al. 1998 *New Astronomy* **3** 539 and *Third Int. Symp. on Sources and Detection of Dark Matter in the Universe*, ed. D. Cline (Amsterdam: Elsevier), in press
- [2] Fichtel C E and Trombka J I 1997 *Gamma-Ray Astrophysics, New Insights into the Universe*, NASA Ref. 1386
- [3] Hunter S D et al. 1997 *Astrophys. J.* **481** 205
- [4] Pohl M and Esposito J A 1998 *Astrophys. J.* **507** 327
- [5] Strong A W, Moskalenko I V and Reimer O 1999 astro-ph/9912102
- [6] Sreekumar P et al. 1998 *Astrophys. J.* **494** 523
- [7] Thompson D J and Fichtel C E 1982 *Astron. Astrophys.* **109** 352
- [8] Stecker F W, Morgan D L and Bredekamp J 1971 *Phys. Rev. Lett.* **27** 1469
- [9] Page D M and Hawking S 1976 *Astrophys. J.* **206** 1
- [10] Cline D 1998 *Astrophys. J.* **501** L1
- [11] Gnedin N Y and Ostriker J P 1992 *Astrophys. J.* **400** 1

† For simplicity, we suppose here that the halo of the Galaxy is spherical and we employ eq. (16) with $f = 1/2$.

- [12] Hartmann D H 1995 *Astrophys. J.* **447** 646
- [13] Jungman G, Kamionkowski M and Griest K 1996 *Phys. Rep.* **267** 195
- [14] Fichtel C E, Simpson G A and Thompson D J 1978 *Astrophys. J.* **222** 833
- [15] Kraushaar W L et al. 1972 *Astrophys. J.* **177** 341
- [16] Strong A W, Wolfendale A W and Worrol D M 1976 *J. Phys. A: Math. Gen.* **9** 1553
- [17] Lichti G G, Bignami G F and Paul J Q 1978 *Astrophys. Space Sci.* **56** 403
- [18] Bignami G F, Fichtel C E, Hartmann R C and Thompson D J 1979 *Astrophys. J.* **232** 649
- [19] Kazanes D and Protheroe J P 1983 *Nature* **302** 228
- [20] Padovani P, Ghisellini G, Fabian A C and Celotti A 1993 *Mon. Not. R. Astron. Soc.* **260** L21
- [21] Stecker F W, Salamon M H and Malkan M 1993 *Astrophys. J.* **410** L71
- [22] Setti G and Woltjer L 1994 *Astrophys. J. Suppl.* **92** 629
- [23] Erlykin A D and Wolfendale A W 1995 *J. Phys. G: Nucl. Phys.* **21** 1149
- [24] Stecker F W and Salamon M H 1996 *Astrophys. J.* **464** 600
- [25] Dar A and Shaviv N J 1995 *Phys. Rev. Lett.* **75** 3052
- [26] Stecker F W and Salamon M H 1997 *Phys. Rev. Lett.* **76** 3878
- [27] Berezhinsky V S, Blasi P and Ptuskin V S 1997 *Astrophys. J.* **487** 529
- [28] De Paolis F, Ingrosso G, Jetzer Ph and Roncadelli M 1995 *Phys. Rev. Lett.* **74** 14
- [29] De Paolis F, Ingrosso G, Jetzer Ph and Roncadelli M 1995 *Astron. Astrophys.* **295** 567
- [30] De Paolis F, Ingrosso G, Jetzer Ph and Roncadelli M 1995 *Comments on Astrophys.* **18** 87
- [31] De Paolis F, Ingrosso G, Jetzer Ph, Qadir A and Roncadelli M 1995 *Astron. Astrophys.* **299** 647
- [32] De Paolis F, Ingrosso G, Jetzer Ph and Roncadelli M 1998 *Astrophys. J.* **500** 59
- [33] De Paolis F, Ingrosso G, Jetzer Ph and Roncadelli M 1999 *Astrophys. J.* **510** L103
- [34] Bahcall N A, Lubin L M and Dorman V 1995 *Astrophys. J.* **447** L81
- [35] Schramm D N and Turner M S 1998 *Rev. Mod. Phys.* **70** 303
- [36] Tytler D, Fan X M and Burles S 1996 *Nature* **381** 207
- [37] Bahcall J N and Casertano S 1985 *Astrophys. J.* **293** L7; Van Albada T S and Sancisi R 1986 *Phil. Trans. R. Soc. Lond.* **A320** 447
- [38] Persic M and Salucci P 1991 *Astrophys. J.* **368** 60
- [39] Maiani L 1979 *Proceedings of the Summer School of Gif-sur-Yvette* **3**; Witten E 1981 *Nucl. Phys.* **B188** 513
- [40] Fall S M and Rees M J 1985 *Astrophys. J.* **298** 18
- [41] Kang H, Shapiro P R, Fall S M and Rees M J 1990 *Astrophys. J.* **363** 488
- [42] Vietri M and Pesce E 1995 *Astrophys. J.* **442** 618
- [43] Ashman K M and Carr B J 1988 *Mon. Not. R. Astron. Soc.* **234** 219
- [44] Ashman K M 1990 *Mon. Not. R. Astron. Soc.* **247** 662
- [45] Fabian A C and Nulsen P E J 1994 *Mon. Not. R. Astron. Soc.* **269** L33
- [46] Nulsen P E J and Fabian A C 1997 *Mon. Not. R. Astron. Soc.* **291** 425
- [47] Kerins E J 1997 *Astron. Astrophys.* **328** 5
- [48] Kerins E J 1997 *Astron. Astrophys.* **332** 709
- [49] Gerhard O E and Silk J 1996 *Astrophys. J.* **472** 34
- [50] Pfenniger D, Combes F and Martinet L 1994 *Astron. Astrophys.* **285** 79
- [51] Sciamia D W 2000 *Mon. Not. R. Astron. Soc.* **312** 33
- [52] Gibson C H and Schild R E 1999 astro-ph/9904366
- [53] Wyithe J S B, Webster R L and Turner E L 1999 *Mon. Not. R. Astron. Soc.* **309** 261

- [54] Palla F, Salpeter E E and Stahler S W 1983 *Astrophys. J.* **271** 632
- [55] Fiedler R L, Dennison B, Johnston K J and Hewish A 1987 *Nature* **326** 675
- [56] Walker M and Wardle M 1998 *Astrophys. J.* **498** L125
- [57] Salati P et al. 1999 *Astron. Astrophys.* **350** L57
- [58] Gyuk G, Dalal N and Griest K 1999 astro-ph/9907338
- [59] Alcock C et al. 2000 astro-ph/0001272
- [60] Gibson B and Mould J 1997 *Astrophys. J.* **482** 98
- [61] Binney J 1998 astro-ph 9809097
- [62] Draine B T 1998 *Astrophys. J.* **509** 41
- [63] De Paolis F, Ingrassio G, Jetzer Ph and Roncadelli M 1998 *Mon. Not. R. Astron. Soc.* **294** 283
- [64] Hansen B 1999 *Astrophys. J.* **520** 680
- [65] Lenzuni P, Chernoff D F and Salpeter E E 1992 *Astrophys. J.* **393** 232
- [66] Kerins E J and Evans N W 1998 *Astrophys. J.* **503** L75
- [67] Taylor J 1998 *Astrophys. J.* **497** L81
- [68] Hansen B 1998 *Nature* **394** 860
- [69] Méndez R A and Minniti D 2000 *Astrophys. J.* **529** 911
- [70] Ibata R et al. 1999 *Astrophys. J.* **524** 95
- [71] Valentijn E A and van der Werf P P 1999 *Astrophys. J.* **522** L29
- [72] López-Corredoira M, Beckman J E and Casuso E 1999 *Astron. Astrophys.* **351** 920
- [73] Berezhinskii V S et al. 1990 *Astrophysics of cosmic rays* (North-Holland, Amsterdam)
- [74] Wdowczyk J and Wolfendale A W 1995 *24th International Cosmic Ray Conference* vol 3 360
- [75] Simpson J A and Connel J J 1998 *Astrophys. J.* **497** L85
- [76] Schlickeiser R, Sievers A and Thiemann H 1987 *Astron. Astrophys.* **182** 21
- [77] Hillas A M 1984 *Ann. Rev. Astron. Astrophys.* **22** 425
- [78] Breitschwerdt D, McKenzie J F and Völk 1991 *Astron. Astrophys.* **245** 79
- [79] Gaisser T K 1990 *Cosmic Rays and Particle Physics* (Cambridge University Press Cambridge)
- [80] Sreekumar P et al. 1993 *Phys. Rev. Lett.* **70** 127
- [81] Völk H J, Aharonian F A and Breitschwerdt D 1996 *Space Sci. Rev.* **75** 279
- [82] Kalberla P M W, Shchekinov Y A and Dettmar R J 1999 *Astron. Astrophys.* **350** L9
- [83] Mori M 1997 *Astrophys. J.* **478** 225
- [84] Dermer C D 1986 *Astron. Astrophys.* **157** 223
- [85] Porter T A and Protheroe R J 1997 *J. Phys. G: Nucl. Phys.* **23** 1765
- [86] Mazzei P, Xu C and De Zotti G 1992 *Astron. Astrophys.* **256** 45
- [87] Cox P and Mezger P G 1989 *Astron. Astrophys. Rev.* **1** 49
- [88] Bloemen H 1989 *Ann. Rev. Astron. Astrophys.* **27** 469
- [89] Ozel M E and Berkhuijsen E M 1987 *Astron. Astrophys.* **172** 378
- [90] Ozel M E and Fichtel C E 1988 *Astrophys. J.* **335** 135
- [91] Sreekumar P et al. 1994 *Astrophys. J.* **426** 105